



Title:

Fabrication of Right Triangular Prism Retroreflectors through $3\frac{1}{2}$ -Axis Ultraprecise Single Point Inverted Cutting

Authors:

Benjamin W. Hamilton, bhamilt8@uwo.ca, Western University, London, Canada

Sama Hussein, sabdelw3@uwo.ca, Western University, London, Canada

O. Remus Tutunea-Fatan, rtutunea@eng.uwo.ca, Western University, London, Canada

Evgueni V. Bordatchev, evgueni.bordatchev@nrc-cnrc.gc.ca, National Research Council, London, Canada

Keywords:

Automotive lighting, retroreflector design, optical performance, $3\frac{1}{2}$ -axis diamond cutting

DOI: 10.14733/cadconfP.2016.246-250

Introduction:

A retroreflector (RR) is an optical device that reflects the light back to the originating source. Two of the most common types of RRs are lens-and-mirror (commonly called cat's eye) and inverted corner cube (ICC). As Fig. 1 implies, while lens-and-mirror RR relies on a mirror to return the incident beam, ICC makes use of its three mutually perpendicular facets to achieve retroreflection. The retroreflective property of these optical elements is speculated in a number of applications including, but not limited to traffic safety, communications, and metrology.

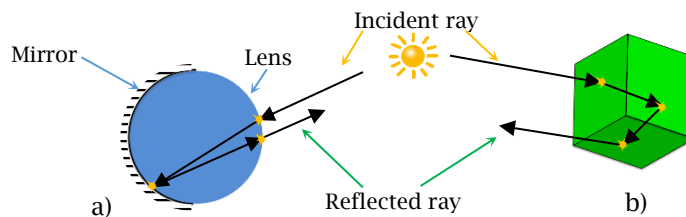


Fig. 1: Typical RR elements: a) lens-and-mirror and b) inverted corner cube.

Automotive industry widely employs ICC RR elements for illumination/lighting purposes, a typical example in this category being represented by the taillights installed on virtually every vehicle. The conventional process of manufacturing ICC RR arrays involves the use of pin-bundling technique, which has been in use for several decades. According to this fabrication method, each RR element of the array is being individually formed by the end of a pin characterized by a hexagonal cross-section and three mutually-orthogonal end faces. Each of the forming face of the pin is manufactured by lapping, in an attempt to attain a qualitatively superior surface. Once individual pins are completed, a group of pins are bundled together and a cavity insert of the entire RR array is created through electroforming. Its inherent complexity makes pin-bundling inefficient, error-prone and difficult to use for microscale features, particularly to the stringent surface quality requirements calling for $R_a < 10$ nm which is commonly equated with optical surface quality. For this reason, more efficient and versatile retroreflector fabrication techniques are highly desirable and two new ideas have recently emerged in this regard: i) development of cutting/machining-based fabrication techniques and ii) development of alternate RR shapes, preferably of lower geometric complexity.

In response to these challenges, a new fabrication process called ultraprecise single point inverted

cutting (USPIC) along with a novel RR geometry coined as right triangular prism (RTP) have been recently developed [3, 4] as viable alternatives to pin-bundling fabrication and ICC RR design, respectively. However, while the initial experiments proved that USPIC can produce the desired RTP geometry [3], it also became clear that the combination of plunging and ploughing motions that can be generated through the sole involvement of the translational axes of a five-axis machine is insufficient to attain the intended optical surface quality. To address this, the primary goal of the current study was to fabricate the new RTP geometry through a combination of translational and rotational motions to represent an enhancement over the previous unidirectional and translational-only approach.

Design and Optical Performance of the RTP Arrays:

Optical Characterization of the RTP Element

To ensure the retroreflective functionality of the novel RTP geometry, its geometry was modeled in CAD and then subjected to optical simulation analysis performed with a specialized software. The geometry of an RTP includes two reflective facets with role in total internal reflection (TIR) and one incident facet/aperture through which light enters and then exits (Fig. 2). According to the automotive use of the RRs, an illumination element whose size is determined by *thickness*, *width* and *base* was joined with of the incident face of the RTP.

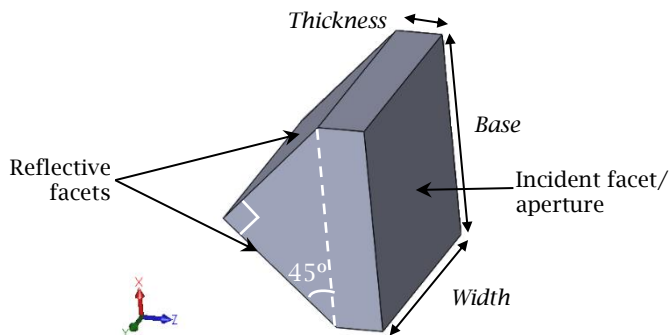


Fig. 2: Geometry of the RTP element.

To assess the optical performance of the new RTP design, the retroreflective efficiency (RRE) – defined as the percentage ratio of retroreflected light to incidence light – was determined through a series of optical simulations in which the primary variable was the direction of the incident beam (Fig. 3). The optical simulation model (Fig. 3a) included an RTP element with a rectangular aperture of 0.45 x 0.45 mm, a light source with a rectangular shape matching that of the RTP aperture, as well as a detector capable to measure the quantity of the retroreflected light. The material assumed for RTP element was polymethyl methacrylate (PMMA).

To verify the retroreflective capabilities of the RTP, the light source was tilted to cover a range of incident angles between -40° and $+40^\circ$ and it was also simultaneously shifted vertically up and down in order to ensure the aforementioned areal matching between RTP's aperture and that of the rectangular-profiled light source. The incoherent irradiance (W/cm^2) of the retroreflected light acquired by the detector was used to calculate the RRE corresponding to 1 W of light projected at various incidence angles. A larger 5° increment was used to scan the -40° to $+40^\circ$ range, while a smaller/finer 1° increment was used between -5° and $+5^\circ$. The results presented in Fig. 3b reveal that as the incidence angle increases, the RRE of the RTP element decreases since more light is lost either because it is reflected at the incident face of the illumination element or because it is never returned in the direction of the observer/detector. As such, the results imply that the best optical performance occurs when RTP's incident face is normal to the incident light. However, this theoretically "ideal" RR may not be in fact suitable for automotive lighting applications as it returns the incident light back to its source whereas this location might or may or may not coincide with the actual position of the observer.

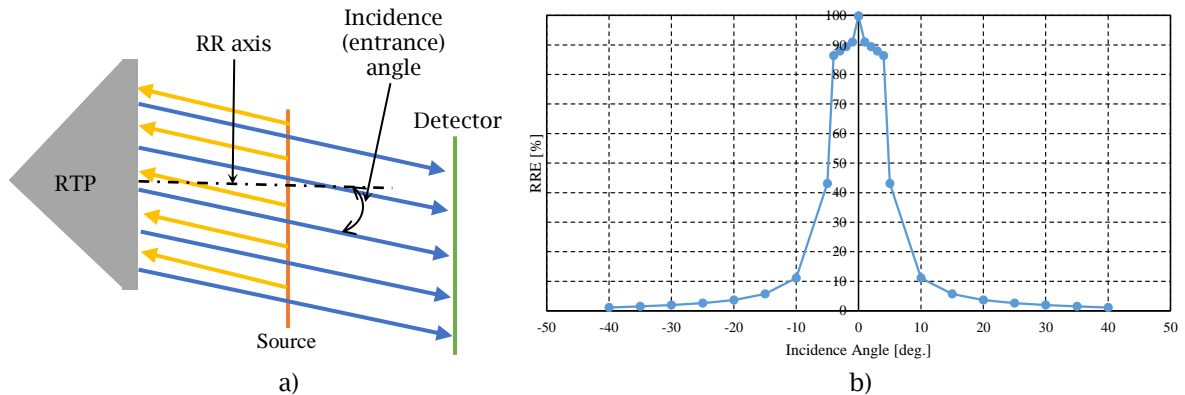


Fig. 3: Optical performance of the RTP: a) optical simulation model, and b) optical simulation results.

Automatic CAD-Based Generation of the RTP Array

Most retroreflective surfaces could be envisioned as arrays of individual RTP elements forming a structured/patterned surface. In general terms, the base surface – in which the optical RTP cavities are fabricated/embedded – could have any freeform shape (such is the case of automotive taillights), but in the context of the current study it was simply assumed as planar. Following this, while many array configurations can be imagined, the one to be examined in this work has assumed a brick-like pattern for the location and orientation of the RTP elements. As shown in Fig. 4, a number of geometrical parameters are required to constrain the topology of the array.

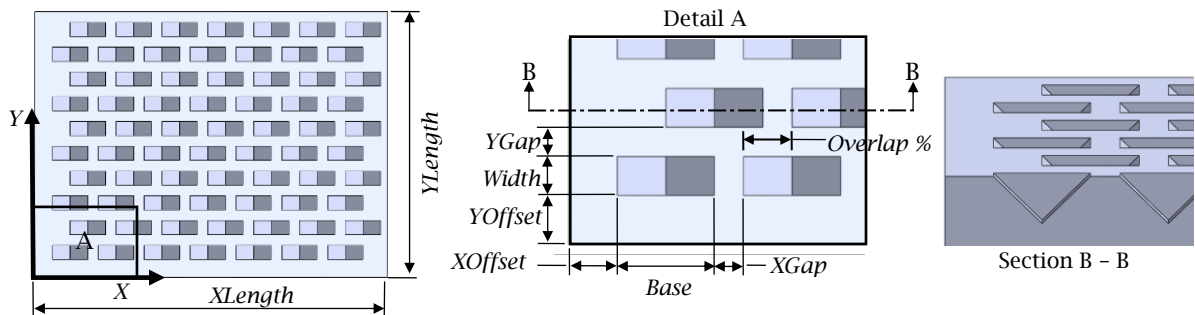


Fig. 4: Geometrical parameters of the RTP array.

To rapidly generate arrays to belong to the same family, a Visual Basic script/macro was created under SolidWorks environment. The program collects all input parameters outlined in Fig. 4 from a text file and then generates the geometry of the RTP array according to the preset design constraints and rules.

Fabrication of the RTP Array through $3\frac{1}{2}$ -Axis Machining:

Diamond Cutting Tool

To fabricate the intended RTP array, a custom tool was developed and manufactured for use in USPIC operations. The cutter consists of a steel shank and a diamond tip and shares many design characteristics with cutting tools used in parting or turning operations, the primary difference being that clearance and rake faces were positioned in a rather reversed manner (Fig. 5). The use of a diamond tip – that is specific to ultraprecise machining operations – is meant to ensure an optical quality on the retroreflective facets of the RTP.

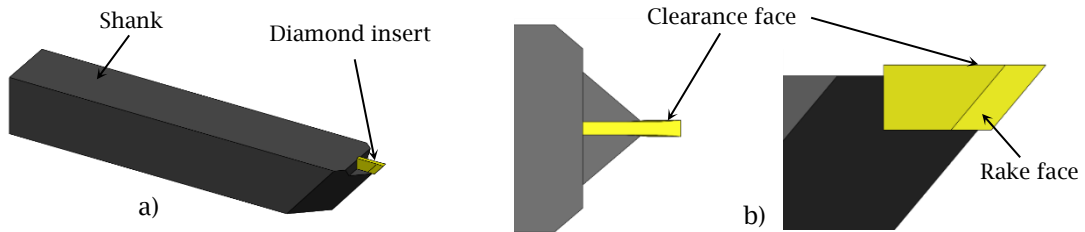


Fig. 5: Design of the diamond cutting tool: a) overview of the cutting tool, and b) constructive detail of the tool tip.

Cutting Motions and Strategies

As described in a previous study [3], depending on the relative position between the tool tip and RTP facet, two principal types of motions exist: plunging and ploughing (Fig. 6). The main difference between plunging and ploughing resides in the large discrepancy between the values of the clearance and rake angles, which in turn affects significantly the quality of the RTP facet being generated. Without entering into details, it will be briefly mentioned here that plunging tends to yield surfaces that are qualitatively superior to those generated through ploughing.

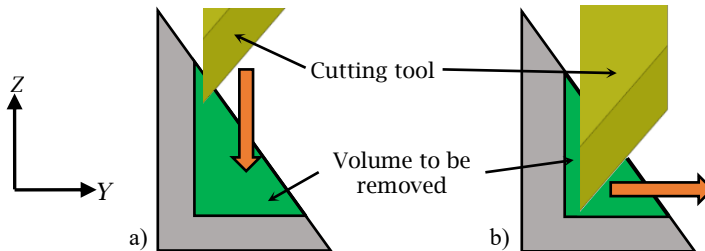


Fig. 6. RTP cutting motions: a) plunging, and b) ploughing.

Furthermore, it is important to note that while a “unidirectional” strategy consisting of a succession of plunging and ploughing motions to generate each of the two RTP facets could be achieved by means of a three-axis CNC machine, this is not the case of the “bidirectional” approach according to which each of the two facets should be finished solely by means of plunging. As such, in order to expose the second RTP facet in an appropriate manner to the cutter, a repositioning of the RTP array is required and this could only be attained through the rotation of the workpiece.

Since the rotary axes of the CNC machine have to move in an intermittent manner and they do not need to move simultaneously with the translational axes, the kinematics of a conventional $3\frac{1}{2}$ -axis machining operation – sometimes also called 3+2, inclined, fixed or tilted machining [1] – as previously demonstrated in milling [2], provides sufficient functionality in the present bidirectional USPIC context. However, since it is unclear whether any of the previously-developed generalized postprocessors [5] – that were primarily intended for five-axis surface milling – were usable in the new USPIC context, it became soon apparent that a need for a custom-build postprocessor exists.

Machine Tool Kinematics

While $3\frac{1}{2}$ -axis machining enables the bidirectional fabrication of the RTP array through an alternation of translational and rotational/indexing motions only, the stringent optical quality requirements prevent in fact the use of a conventional three-axis machine that was simply retrofitted with an indexing table. As such, a state-of-the-art five-axis CNC micromachining center with rotary table (e.g. CA) configuration with triple head functionality (e.g. milling, laser cutting and probing) has been altered to allow the attachment of the diamond cutting tool in a vertical direction that is positioned laterally with respect to main spindle of the machine (Fig. 7a). By following the procedure detailed in [6] a complete inverse kinematic model of the five-axis machine has been developed.

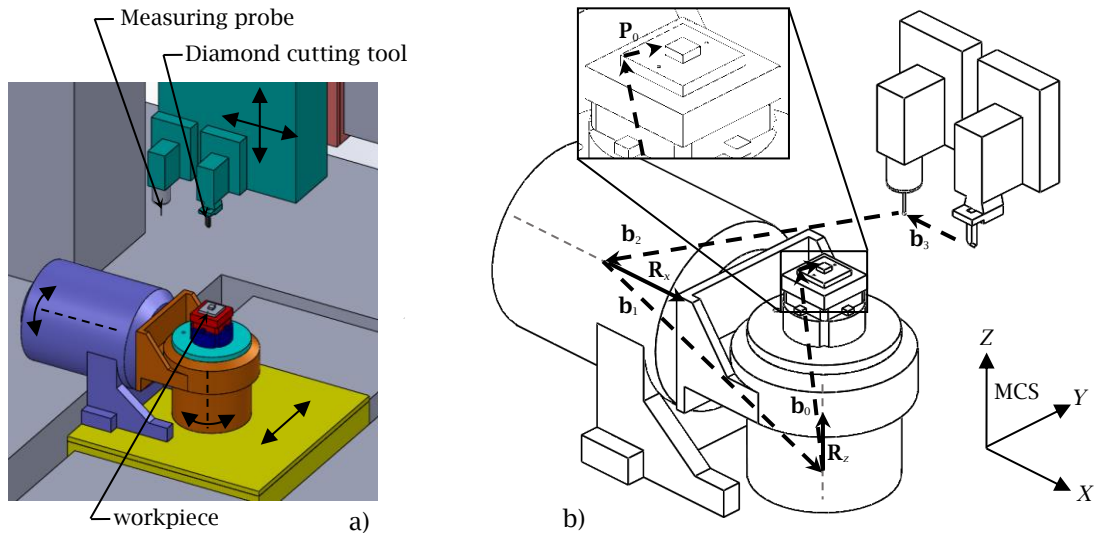


Fig. 7: Five-axis machine tool used in $3\frac{1}{2}$ -axis USPIC operation: a) kinematic motions, and b) development of the inverse kinematics model.

Results and Conclusions:

Once the inverse kinematic model of the five-axis machine was completed and tested, calibration procedures were used to determine the position vectors \mathbf{b} (Fig. 7b) as well as the misalignment between the C and A axes of the machine tool and Z and X axes of the fixed in space machine coordinate system (MCS). As a final step of the study, a sample RTP array was cut to demonstrate the feasibility of the proposed $3\frac{1}{2}$ -axis USPIC technique. The evaluations of the surface quality performed so far have confirmed the enhancements brought by the new bidirectional approach over the previously-proposed unidirectional cutting technique.

Acknowledgements:

The work presented in this study is the result of the collaboration between Western University and National Research Council of Canada. Partial financial support was also provided by NSERC.

References:

- [1] Albert, M.: An Overview of 3+2 Machining, *Modern Machine Shop*, 79, 2006, 94-97. <http://www.mmsonline.com/articles/an-overview-of-3-2-machining>
- [2] Chen, Z.C.; Dong, Z.; Vickers, G.W.: Automated Surface Subdivision And Tool Path Generation For $3\frac{1}{2}$ -Axis CNC Machining Of Sculptured Parts, *Computers in Industry*, 50, 2003, 319-331. [http://dx.doi.org/10.1016/S0166-3615\(03\)00019-8](http://dx.doi.org/10.1016/S0166-3615(03)00019-8)
- [3] Hamilton, B.; Hussein, S.; Tutunea-Fatan, O.R.; Bordatchev, E.V.: Fabrication of Right Triangular Prism Retroreflectors through Ultraprecise Single Point Inverted Cutting, paper MSEC2016-8857, accepted to ASME MSEC 2016 conference to be held in Jun. 2016 in Blacksburg, VA.
- [4] Hussein, S.; Hamilton, B.; Tutunea-Fatan, O.R.; Bordatchev, E.V.: Novel Retroreflective Micro-Optical Structure for Automotive Lighting Applications, *SAE International Journal of Passenger Cars - Mechanical Systems* 9(2), 2016. <http://dx.doi.org/10.4271/2016-01-1407>
- [5] She, C.; Chang, C.: Design of a generic five-axis postprocessor based on generalized kinematics model of machine tool, *International Journal of Machine Tools & Manufacture*, 47, 2007, 537-545. <http://dx.doi.org/10.1016/j.ijmachtools.2006.06.002>
- [6] Tutunea-Fatan, O.R.; Feng, H.Y.: Configuration analysis of five-axis machine tools using a generic kinematic model, *International Journal of Machine Tools and Manufacture*, 44, 2004, 1235-1243. <http://dx.doi.org/10.1016/j.ijmachtools.2004.03.009>